Developmental Cell, Vol. 4, 941–952, June, 2003, Copyright ©2003 by Cell Press

# Asymmetric Distribution of Nuclear Pore Complexes and the Cytoplasmic Localization of β2-Tubulin mRNA in *Chlamydomonas reinhardtii*

**Daniel A. Colón-Ramos,[1,4] Jeffrey L. Salisbury,[2] Mark A. Sanders,[2,5] Shailesh M. Shenoy,[3] Robert H. Singer,[3] and Mariano A. García-Blanco[1,*]**

[1]Department of Molecular Genetics and Microbiology and
Department of Medicine
Duke University Medical Center
Durham, North Carolina 27710
[2]Tumor Biology Program
Mayo Clinic
Rochester, Minnesota 55905
[3]Department of Cell Biology and
Department of Anatomy and Structural Biology
Albert Einstein College of Medicine
Yeshiva University
1300 Morris Park Avenue
Bronx, New York 10461

## Summary

**Although it is generally accepted that nuclear architecture is an important determinant of nuclear activity, it is not clear whether cytoplasmic events, such as transcript localization and cell polarity, are affected by this architecture. Characterization of the nuclear architecture of the single-cell alga *Chlamydomonas reinhardtii* revealed a polarized nucleus, with nuclear pore complexes preferentially concentrated at the posterior side of the nucleus. Nuclear asymmetry was greatly exaggerated during the upregulation of genes encoding flagellar proteins, when nuclear pore complexes (NPCs) were observed to hyperpolarize to the posterior side of the nucleus while heterochromatin polarized to the anterior side. Interestingly, prior to deflagellation, the β2-tubulin gene was preferentially located in the posterior region of the nucleus, and following deflagellation, β2-tubulin transcripts accumulated posteriorly in polysome-rich cytoplasmic regions adjacent to the highest concentration of NPCs, suggesting a connection between nuclear architecture and cytoplasmic transcript localization.**

## Introduction

The nucleus is highly compartmentalized into functional subnuclear domains (reviewed in Dundr and Misteli, 2001). The most prominent of these is the nucleolus, which consists of an assembly of rRNA gene repeats and rRNA and proteins involved in the synthesis, processing, and assembly of ribosomal subunits (García-Blanco et al., 1995; Leger-Silvestre et al., 1999). Other nucleoplasmic compartments, such as the Cajal, Gemini, and PMN bodies, define nuclear compartments with distinct gene, transcript, and protein composition (reviewed in Dundr and Misteli, 2001; Gall, 2001). In addition, chromosomes occupy distinct territories within the nucleus (Marshall et al., 1996).

Nuclear architecture has significant effects on transcription and processing of nascent transcripts. Nuclear complexes containing RNA polymerase II localize to sites of gene transcription, and splicing factor complexes (SFCs) localize as nuclear "speckles" to distinct domains separated from sites of transcription (reviewed in Dundr and Misteli, 2001). Additionally, cotranscriptional processing such as capping, splicing, and polyadenylation occurs within the vicinity of active gene transcription, implicating nuclear architecture in the regulation of transcript processing (reviewed in Goldstrohm et al., 2001 and Maniatis and Reed, 2002; Zhang et al., 1994).

Whereas these observations suggest that nuclear architecture affects gene expression, it is not clear whether nuclear organization is linked to cytoplasmic events such as transcript targeting and cell polarity. For example, whereas mRNA stability and cytoplasmic localization depend on nuclear factors (reviewed in Brennan and Steitz, 2001; Gu et al., 2002; Long et al., 2001), there is little evidence to directly link nuclear architecture with the cytoplasmic fate of transcripts. Blobel's "gene gating" hypothesis suggested that cytoplasmic localization of new transcripts may result from directed nucleocytoplasmic transport, such that active genes located near the nuclear periphery, adjacent to the nuclear pore complexes (NPCs), may help target the mRNA to its cytoplasmic destination (Blobel, 1985). Although certain active genes have been found near the nuclear periphery, their localization has not been found to influence gene activity or cytoplasmic transcript localization (Bullock and Ish-Horowicz, 2001; Lawrence et al., 1989; Mahy et al., 2002; Wilkie et al., 1999).

In the present study, we used *Chlamydomonas reinhardtii*, a biflagellated unicellular alga with an asymmetric cellular structure to study the relationship between nuclear architecture and cytoplasmic processes. Cellular asymmetry in *Chlamydomonas* is determined by the anterior position of the flagella and the posterior position of the chloroplast, with the nucleus nested between these two conspicuous organelles (Harris, 1989; see also Figures 1 and 2A). The nucleus is about 3–5 μm in diameter and is surrounded by a double nuclear membrane envelope interrupted by numerous nuclear pores (~500 Å in diameter; Johnson and Porter, 1968; Sager and Palade, 1957; Weiss et al., 2000). A spherical nucleolus consisting of tightly packed particles surrounding finer particles and light inclusions is located near its center (Harris, 1989; Holmes and Dutcher, 1989; Johnson and Porter, 1968; see also Figure 1). The *C. reinhardtii* nucleus is tethered to the two basal bodies and the flagella by a cytoskeletal fiber complex known as the nucleus-basal body connector (NBC) that contains the calcium binding protein centrin (20 kDa; Wright et al., 1985). We previously reported that contraction of the

*Correspondence: garci001@mc.duke.edu
[4]Present address: University Program in Genetics, Duke University, Durham, North Carolina 27710.
[5]Present address: College of Biological Sciences, University of Minnesota, St. Paul, Minnesota 55108.

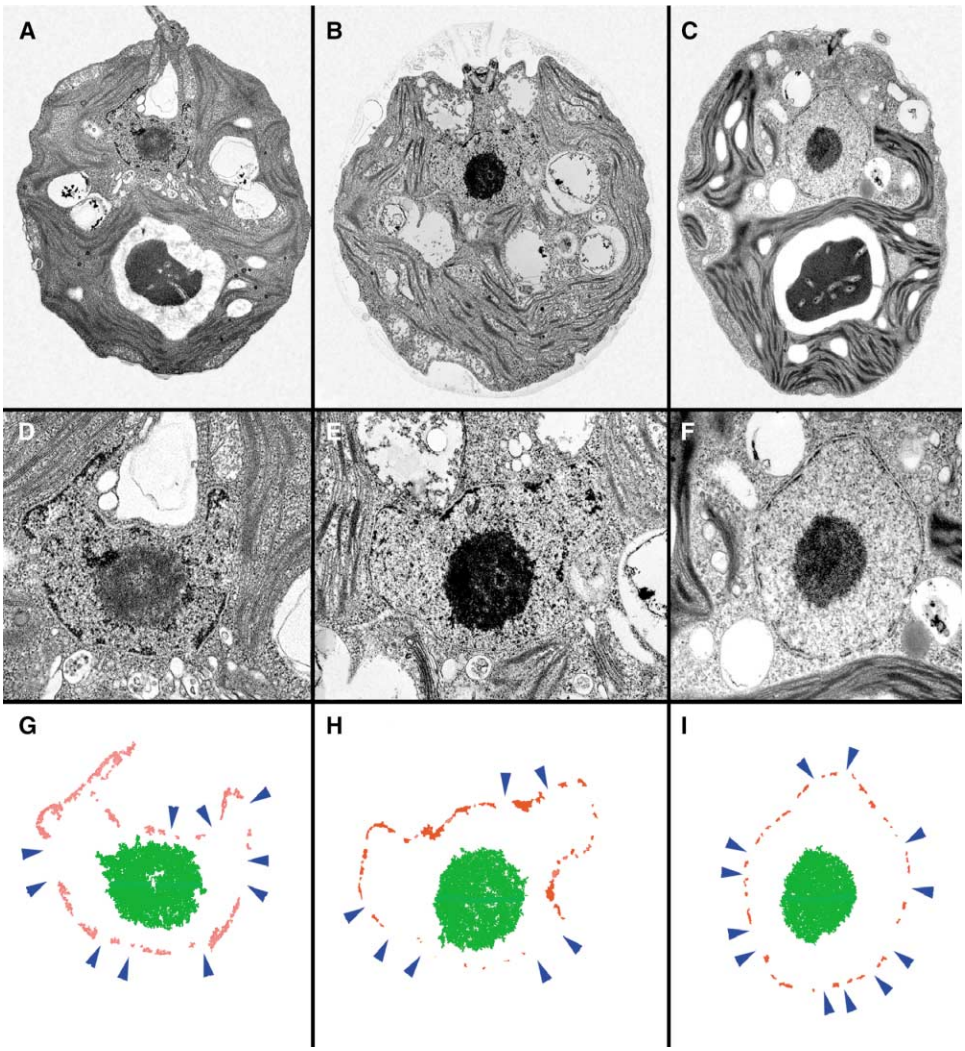


Figure 1. Flagellar Excision Leads to Asymmetric Distribution of Heterochromatin

Electron micrographs of medial longitudinal sections of *Chlamydomonas reinhardtii* before (A), immediately following (B), and 90 min after (C) pH shock-induced flagellar excision. Note that the distance between the nucleus and flagellar apparatus is reduced at the time of flagellar excision (B) and the nucleus has undergone a subtle shape change. Higher magnification of nuclear profiles (D–F) shows a redistribution of heterochromatin immediately adjacent to the nuclear envelope. Before flagellar excision (D), heterochromatin is uniformly dispersed in patches around the nuclear periphery. Immediately following flagellar excision (E), heterochromatin has redistributed toward the flagellar apparatus and becomes cleared from the posterior side of the nucleus. By 90 min of recovery from pH shock (F), heterochromatin has redistributed to again show a relatively even distribution around the nuclear periphery. At the 90 min time point, the heterochromatin at the nuclear envelope appears to be somewhat reduced in thickness. Diagrammatic representation (G–I) of the redistribution of heterochromatin (red) and location of nuclear pores (blue arrowheads) seen in the micrographs illustrated in (D–F) is shown.

NBC following deflagellation causes a dramatic change in nuclear shape (from oval to pyriform or pear-shaped) and its displacement toward the anterior end of the cell (Salisbury et al., 1987; Wright et al., 1985). Others have shown that following deflagellation there is a dramatic upregulation of genes encoding flagellar proteins required for the complete regeneration of the flagella (Baker et al., 1984; Keller et al., 1984). In this study, we explored changes in nuclear architecture following deflagellation using electron microscopy and confocal immunofluorescence, which allowed simultaneous visualization of the NPCs, the core (Sm) snRNP proteins, the nucleolus, and the nucleus-basal body connector. We also used fluorescent in situ hybridization to visualize the location of the β2-tubulin gene and the cytoplasmic localization of β2-tubulin transcripts. We found that NPCs were asymmetrically distributed toward the posterior pole of the *Chlamydomonas* nucleus. This asymmetry in NPC distribution was greatly exaggerated following deflagellation, when dramatic changes in overall nuclear shape and redistribution of heterochromatin near the nuclear envelope was also observed. Importantly, newly synthesized β2-tubulin transcripts were localized in the posterior cytoplasm adjacent to the nu-

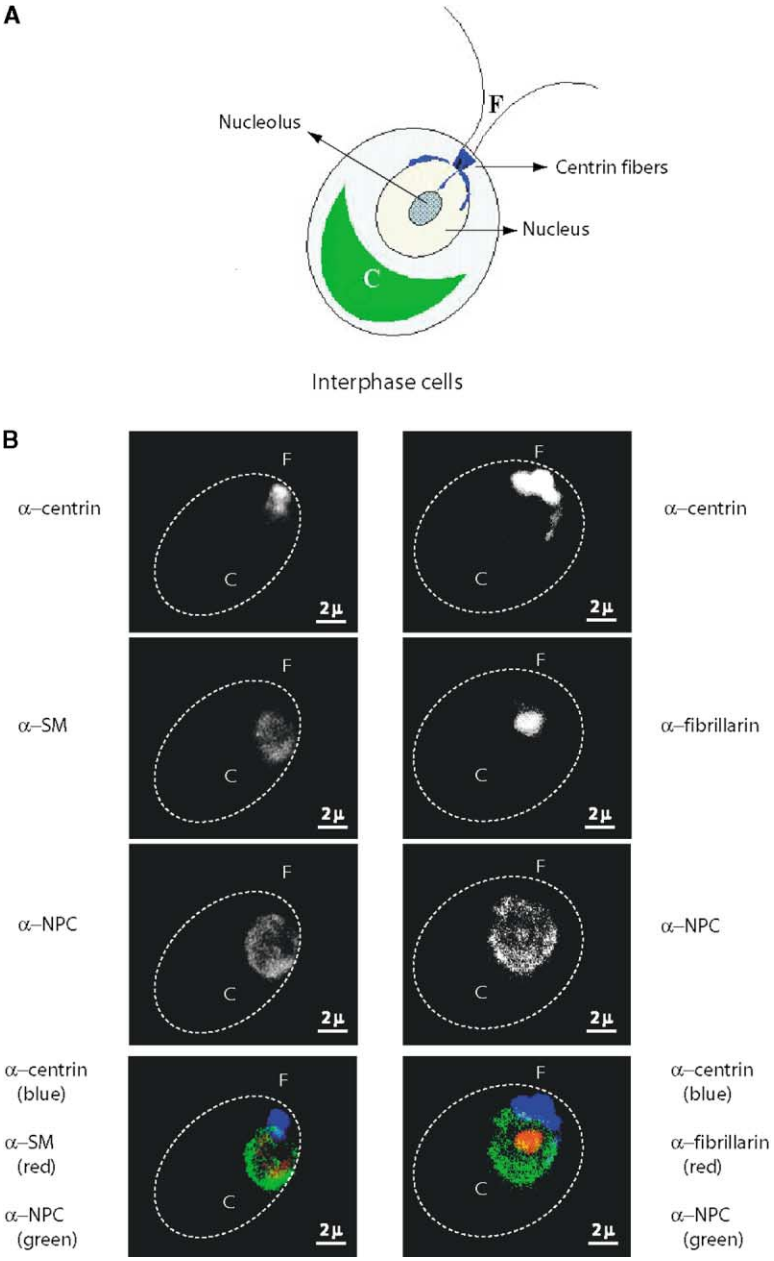


Figure 2. Nuclear Architecture in Interphase Cells

(A) Diagram of the nuclear architecture of *C. reinhardtii* cells in the context of the rest of the cellular structure (based on studies conducted by Johnson and Porter, 1968; Salisbury et al., 1987; Schotz et al., 1972; Weiss et al., 2000; also discussed in Harris, 1989). The *Chlamydomonas reinhardtii* nucleus (clear) is nested between the two flagella at the anterior end (F) and the chloroplast at the posterior end ([C], in green). The flagella are connected to the nucleus via the nucleus-basal body connector, which contains centrin fibers (blue). The spherical nucleolus (dotted) has been previously visualized in electron microscopy studies.

(B) Triple confocal immunofluorescence was conducted in interphase *C. reinhardtii* cells using antibodies against centrin fibers (blue), the core Sm proteins of spliceosomal snRNPs (red), nucleolar fibrillarin (red), and NPC proteins (green). Dotted lines outline the cell wall, which was visualized by differential interference contrast (DIC) microscopy. For convenience and comparison, the cells were placed in the same orientation as the diagram, with anterior facing up (F, flagellum) and the posterior end facing down (C, chloroplast).

clear area with the highest NPC density. Thus, these observations suggest that an asymmetric and dynamic nuclear architecture can affect transcript localization in the cytoplasm.

## Results

### Heterochromatin Redistribution during Flagellar Regeneration

*C. reinhardtii* sheds its flagella when exposed to adverse environmental conditions, such as pH change, through an active process known as flagellar excision or autotomy (Rosenbaum et al., 1969). Upon return to favorable conditions, cells regenerate their flagella within 2 hr following increased transcription and stability of mRNAs coding for flagellar proteins (Baker et al., 1984, 1986; Bernstein et al., 1994; Keller et al., 1984; Schloss et al., 1984). In order to determine whether the nuclear architecture was affected during this process of increased transcription activity, we analyzed electron micrographs of medial longitudinal sections of *C. reinhardtii* before, immediately following, and 90 min after pH shock-induced flagellar excision.

In undisturbed cells, the nucleus showed a centrally positioned nucleolus and a narrow rim of heterochromatin evenly distributed near the nuclear periphery, just beneath the nuclear envelope (Figures 1A, 1D, and 1G). NPCs appeared to be asymmetrically localized toward the posterior of the nucleus. Immediately following deflagellation, the nucleus became pyriform in shape and

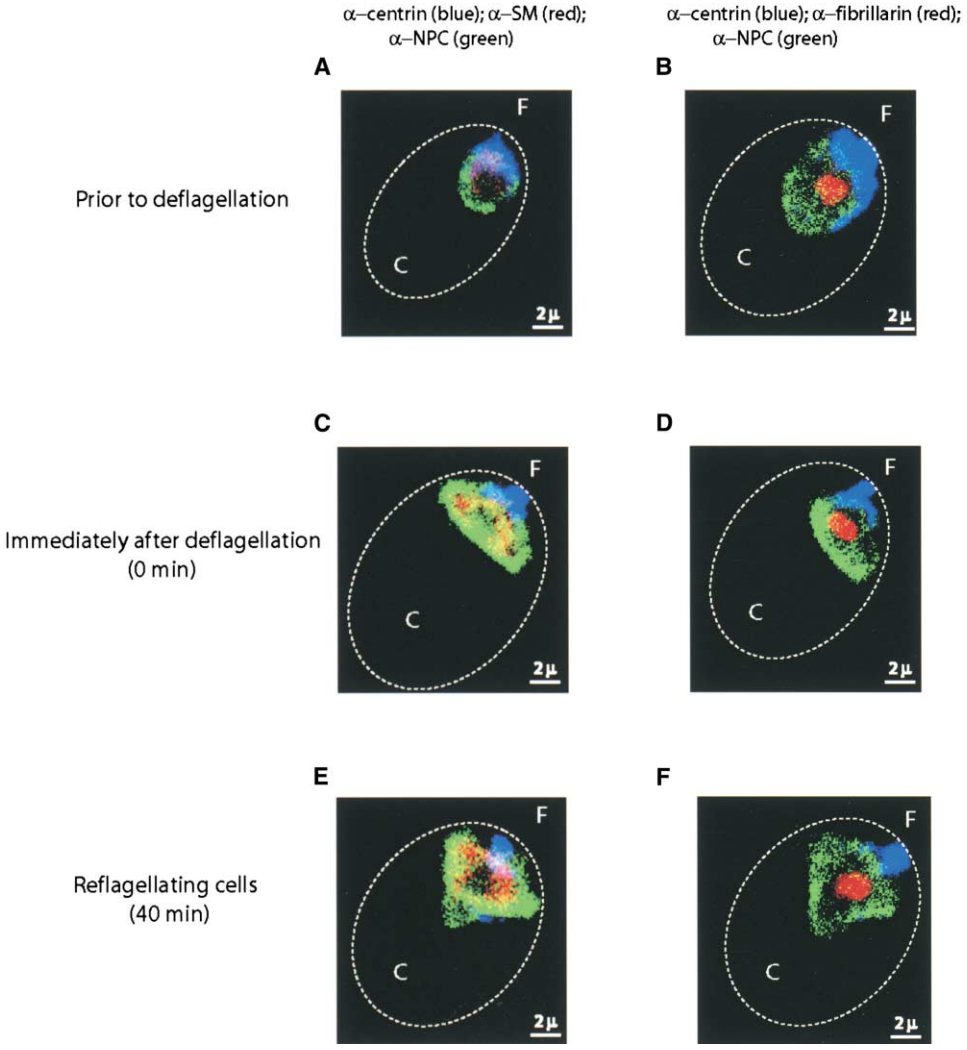


Figure 3. Changes in Nuclear Architecture during Flagellar Regeneration

Cells were deflagellated by pH shock, and allowed to recover in neutral pH media. Samples were collected during recovery and flagellar regeneration. Triple confocal immunofluorescence as described above was carried to visualize changes in nuclear architecture. The anterior end of the cells is labeled F for flagellum, and the posterior part is labeled C for chloroplast.

(A and B) Cells visualized prior to flagellar autotomy.

(C and D) Cells visualized immediately after pH shock.

(E and F) Reflagellating cells visualized 40 min after pH shock.

was displaced toward the flagellar apparatus as previously reported (Salisbury et al., 1987; Wright et al., 1985). A dramatic redistribution of heterochromatin was also apparent in nuclei following deflagellation, such that the narrow rim of heterochromatin near the nuclear envelope appeared to be displaced toward the anterior side of the nucleus (Figures 1B, 1E, and 1H). Interestingly, the asymmetric distribution of the NPCs toward the posterior side of the nucleus noted in unperturbed cells became more pronounced immediately following deflagellation and in cells during the period of flagellar regrowth (Figures 1B, 1E, and 1H).

By about 90 min following deflagellation, cells fully recovered full-length flagella and showed an even distribution of the heterochromatin rim near the nuclear envelope. Whereas NPCs remained concentrated toward the posterior end of the nucleus, their asymmetric distribution was not as pronounced as in cells immediately following deflagellation (Figures 1C, 1F, and 1I).

### NPCs Are Asymmetrically Distributed in *C. reinhardtii* Nuclei

In order to confirm and extend the electron microscope observations, we used immunofluorescence and confocal microscopy to visualize nuclear proteins known to localize in distinct subnuclear compartments. In this study, we utilized mAb 414 antibody (BabCO), a monoclonal antibody that recognizes the nucleoporins (Nup), protein components of the NPC; a human antiserum (AW) against the core Sm protein of the spliceosomal snRNPs (Lerner et al., 1981); and a human antiserum against the nucleolar protein fibrillarin (Ochs et al., 1985).

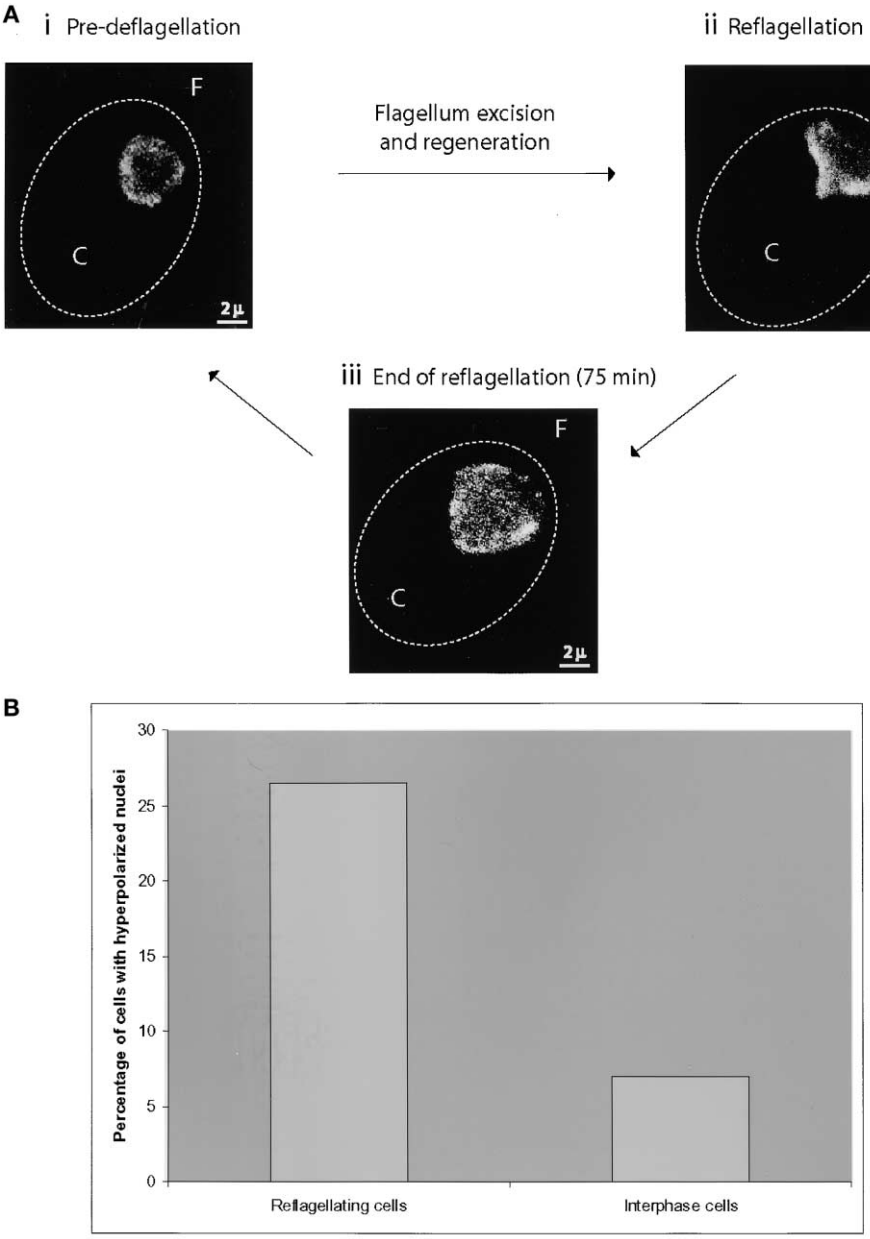


Figure 4. NPC Hyperpolarization during Flagellar Regeneration

Qualitative comparisons of reflagellating cells suggested that there was a marked difference between the NPC distribution in reflagellating cells versus untreated cells (prior to pH shock and recovery).

(A) Panel i: Confocal immunofluorescence of NPC proteins in an untreated cell.

Panel ii: Confocal immunofluorescence of NPC proteins in a reflagellating cell 20 min after pH shock. Within 20 min after flagellar autotomy, many cells where the nucleus had collapsed against the anterior end displayed a posterior nuclear protuberance. Three-dimensional reconstruction showed that the protrusion was not symmetric: it did not expand dorso-ventrally across the posterior end of the nucleus, and was instead present at one side of the nucleus. At 40 and 60 min after deflagellation, we observed populations of cells with intermediate morphology between this contracted nucleus and the oval-shaped, interphase nucleus (see also Figures 3E and 3F). These intermediate nuclei displayed a rhomboid morphology. These observations suggested that the posterior nuclear protuberance and the rhomboid morphology mark the initial stages of the nuclear translocation back to its original shape and position.

Panel iii: Confocal immunofluorescence of NPC proteins in a recovering cell 75 min after pH shock.

(B) Quantification of cells with a hyperpolarized nucleus in untreated versus reflagellating cells. NPC concentration in the anterior and posterior end of 27 untreated cells, versus 34 reflagellating cells, was measured, and the anterior-posterior ratio was calculated. Those cells that had a 40% higher concentration at the posterior versus the anterior end were considered hyperpolarized cells. Of the reflagellating cells, 26.5% had a hyperpolarized nucleus, as compared to 7% of untreated cells.

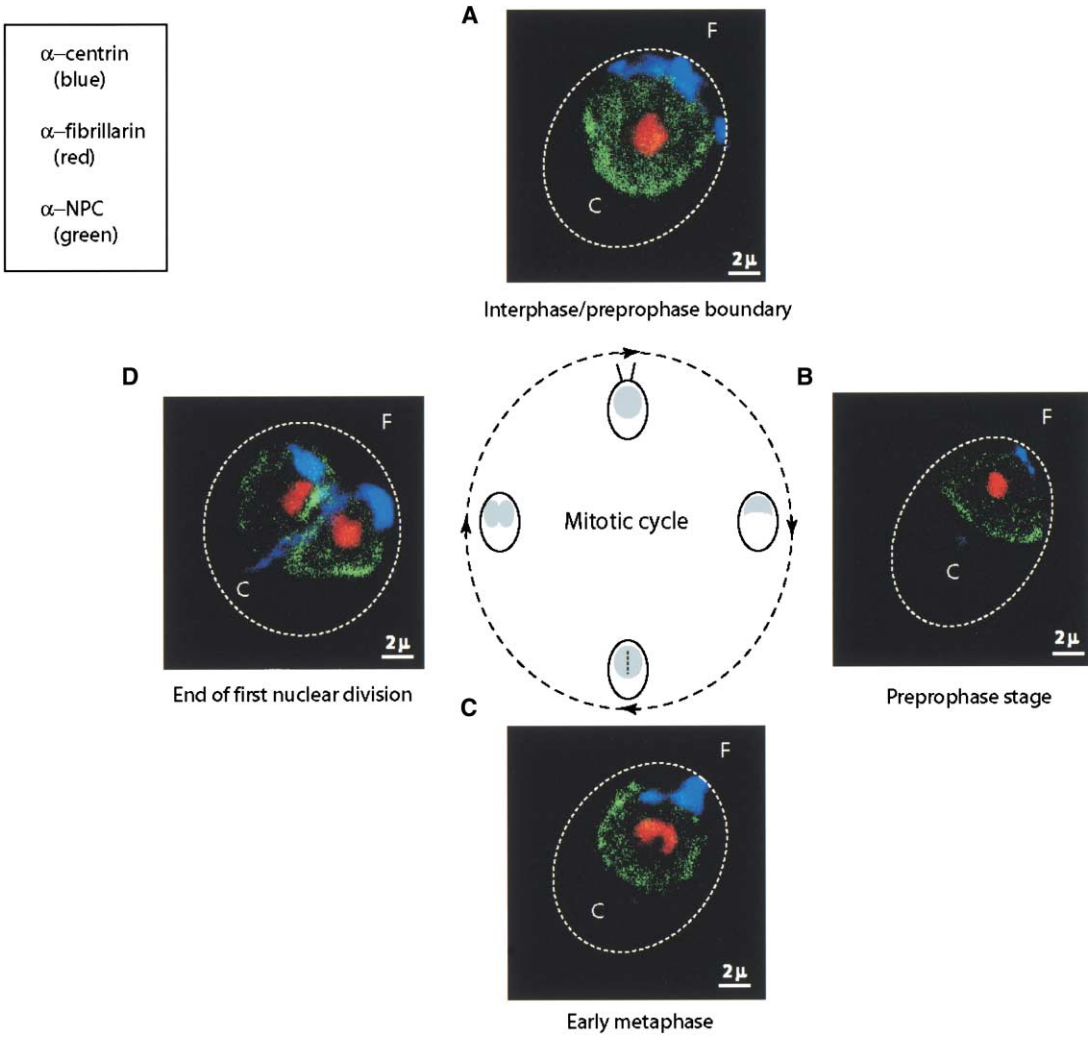


Figure 5. Flagellar Excision Per Se Does Not Lead to NPC Hyperpolarization

Cells were synchronized in a 10 hr dark/14 hr light cycle, and samples were collected during mitosis and cytokinesis. Triple confocal immunofluorescence as described above was performed on the cells to visualize subnuclear compartments. NPCs are represented in green, nucleoli in red, and centrin fibers in blue.

(A) A cell in the interphase/preprophase boundary, just prior to mitosis.

(B) A cell in the preprophase stage, the beginning of mitosis, just after physiological flagellar autotomy.

(C) A cell in early metaphase.

(D) A cell at the end of the first mitotic division. *C. reinhardtii* undergoes two or more mitotic cycles before the daughter cells break free from the mother cell wall that encapsulates them. The dividing cells lose their flagella at the beginning of the mitotic cycle (preprophase stage; Johnson and Porter, 1968; also discussed in Harris, 1989). The nuclear envelope, as previously reported (Johnson and Porter, 1968), did not break down during mitosis, and the nucleolus did not change shape or position, remaining near the center of the nucleus throughout the mitotic cycle. Previous electron microscopic studies of mitotic nuclei reported that the nucleolus disintegrated during mitosis, with its components becoming dispersed throughout the nucleoplasm (Johnson and Porter, 1968). Our immunofluorescence studies did not support this: we did not observe a breakdown of nucleolar structure as defined by anti-fibrillarin staining. During the initial stages of mitosis, the nucleolus increased in size to occupy at least twice as much volume as the interphase nucleolus, became positioned at the axis of nuclear fission, divided, and segregated with the two daughter cells (C and D).

Western blot analysis of *C. reinhardtii* lysates was used to confirm antibody specificity: the Nup 414 antibody specifically recognized four major bands in *C. reinhardtii* lysates: 75 kDa, 60 kDa, 57 kDa, and 45 kDa proteins (data not shown). Although no NPC proteins have been described for *C. reinhardtii*, the size of these proteins in Western blots of *C. reinhardtii* lysates corresponds to the size reported for nucleoporins in yeast and humans (reviewed in Ryan and Wente, 2000). The AW human antiserum, which recognizes the core Sm protein of the spliceosomal snRNP, identified a prominent 22 kDa band and a lighter 27 kDa band (data not shown), similar in size to the 28 kDa B and the 29 kDa B′ snRNP human proteins (Lerner et al., 1981).

In addition, we used a rabbit polyclonal antibody against *C. reinhardtii* centrin to visualize the nucleus-basal body connector (Salisbury et al., 1984; Wright et al., 1985), which also allowed us to locate the nucleus with respect to the flagella and the chloroplast (Figure 2A). The nucleus was also visualized using DAPI (data

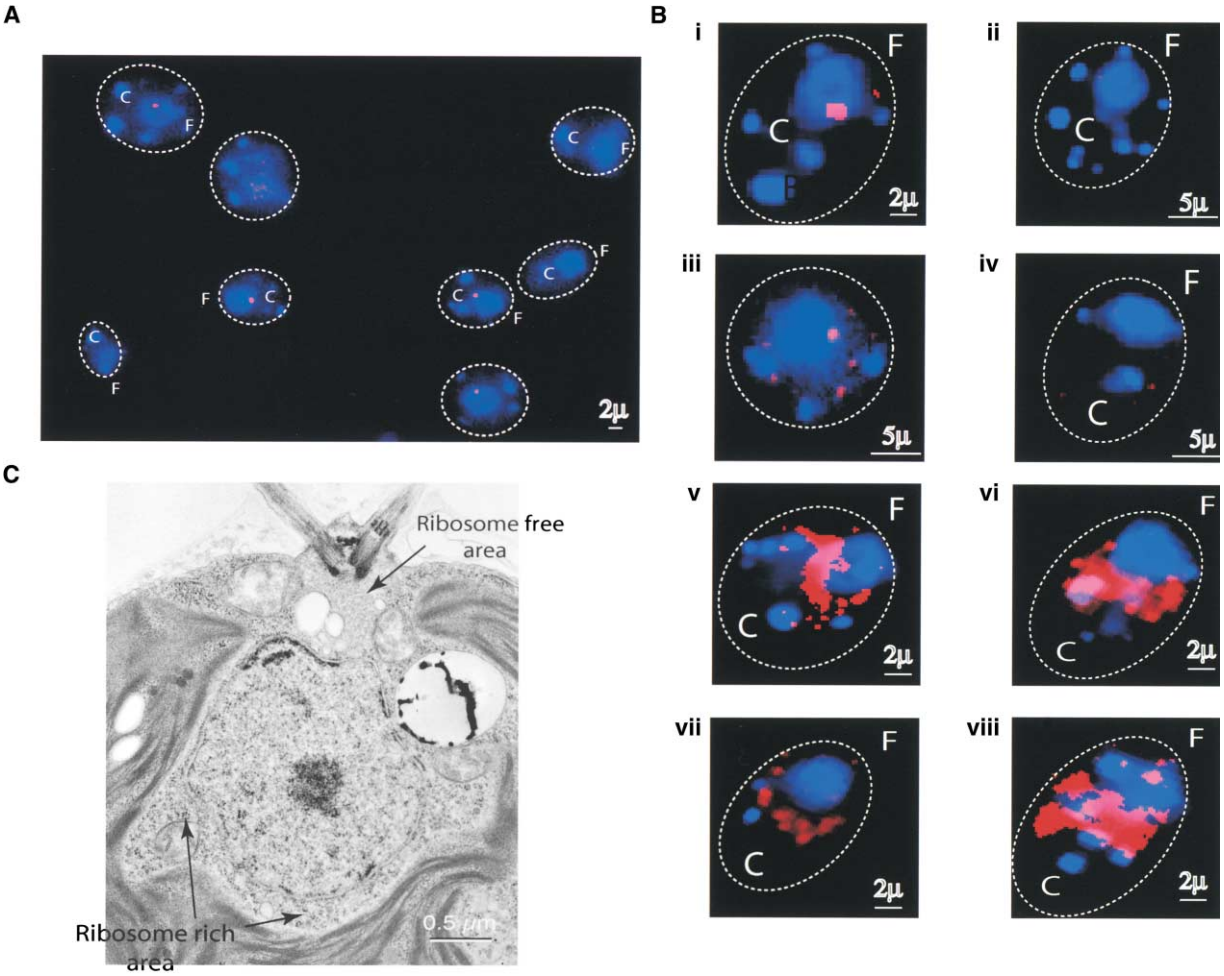


Figure 6. β2-Tubulin Transcripts Localize to the Polysome-Rich Cytoplasmic Area Adjacent to the Posterior End of the Nucleus during Flagellar Regeneration

FISH was conducted against *C. reinhardtii* cells as indicated in the Experimental Procedures. DAPI signals are represented in blue, FISH signals are represented in red.

(A) A field of cells prior to deflagellation, hybridized with β2-tubulin probes.

(B) Panel i: Deconvolved image of an unmanipulated cell hybridized with β2-tubulin probes. Deconvolution removed and reassigned scattered light to its point sources, enhancing signal within the image volume that was then visualized in three dimensions, permitting the digital analysis of the spatial position of the transcription sites/transcripts.

Panel ii: Deconvolved image of an unmanipulated cell hybridized with LacZ probes.

Panel iii: A cell 40 min after deflagellation, hybridized with β2-tubulin probes.

Panel iv: Deconvolved image of a cell 40 min after deflagellation, hybridized with LacZ probes.

Panels v–viii: Deconvolved images of cells 40 min after deflagellation, hybridized with β2-tubulin probes.

(C) Electron micrograph of a medial longitudinal section of *Chlamydomonas reinhardtii*, showing ribosome-rich areas at the cytoplasmic site adjacent to the posterior hemisphere of the nucleus. Polysomes were visualized as tightly packed dark particles.

not shown; see below). Triple confocal immunofluorescence analysis of interphase cell nuclei using these antibodies allowed us to characterize the distribution of the NPCs at the nuclear envelope, the spliceosomal snRNPs, and the nucleoli, and their position relative to the flagellar apparatus and chloroplast (Figure 2B). As previously reported, interphase nuclei are oval shaped, slightly wider at the posterior or chloroplast end (Figure 2C), and narrower at the anterior or flagellar end (Figure 2F), where they attach to the centrin fibers (Salisbury et al., 1988; Figure 2B). Nup 414 staining corroborated our EM observations showing that NPCs were asymmetrically distributed in the nuclear envelope: NPC staining was consistently higher at the posterior pole of the nuclei (Figure 2B). In order to determine whether this distribution was due to the shape of the nucleus, we analyzed optical Z-sections acquired by confocal microscopy. Analysis of the three-dimensional reconstruction demonstrates that the asymmetric distribution of NPCs toward the posterior region of the nucleus was not simply due to nuclear geometry (data not shown). Quantification of NPC staining showed that, on average, there were 20% more NPCs localized to the posterior side of the nucleus as compared to the anterior side, suggesting a genuine nuclear structural asymmetry.

We tested whether other nuclear structures also showed asymmetry in *C. reinhardtii* nuclei. Although we did not observe the typical "speckled" snRNP pattern

described for nuclei of some mammalian cell lines (Lerner et al., 1981), snRNP proteins were found to localize in a compartment that appeared as a granular ring in cross-sections (Figure 2B). The ring staining did not extend to the nuclear envelope, suggesting that there was, as in the case of other eukaryotes, a cortical lamina, which unfortunately we could not visualize with several anti-lamin antisera. Interestingly, the snRNPs were completely excluded from the center of the nucleus, suggesting a centrally located nucleolus. Indeed, anti-fibrillarin antisera stained the central nucleolus precisely in the nuclear region that excluded snRNP staining, consistent with our electron micrograph observations (Figures 1 and 2B). These observations suggest that the nucleolus and the snRNP compartment did not have the same asymmetric distribution observed for NPCs.

### NPCs Hyperpolarize during Flagellar Regeneration

Electron microscopy demonstrated dramatic changes in nuclear architecture following deflagellation and during flagellar regrowth. In order to examine these changes in more detail, we stained nuclei in cells following deflagellation and during flagellar regrowth by triple confocal immunofluorescence using the antibody cocktail described above. Consistent with previous reports (Salisbury et al., 1987; Wright et al., 1985), flagellar autotomy was immediately followed by a contraction of the centrin fibers and movement of the nucleus toward the anterior of the cell (Figures 3A–3D). The movement of the nucleus is accompanied by a dramatic change in nuclear shape: the posterior side of the nucleus was flattened, resulting in a pyriform shape (Figures 3C and 3D). The snRNP-containing nucleoplasm and the nucleolus also became distorted by the dramatic anterior-posterior shortening of the nucleus (Figures 3C and 3D). The movement and change in nuclear shape resulted in a relative increase in the surface area at the posterior side of the nucleus.

The most dramatic difference noted during reflagellation was the hyperpolarization of the NPCs to the posterior nuclear hemisphere (Figure 4A). These results confirmed the EM observations that NPC hyperpolarization was more dramatic in cells following deflagellation and during flagellar regrowth as compared to untreated cells. In order to quantify this difference, we counted the number of untreated and reflagellating cells with hyperpolarized nuclei, which we defined as nuclei with 40% higher NPC concentration at the posterior side of the nucleus. Twenty minutes after pH shock (deflagellation), 26.5% of cells were hyperpolarized, as compared to 7% in untreated cells (Figure 4B). These changes in NPC polarity, combined with the reorganization of heterochromatin, suggested that the nucleus in *C. reinhardtii* became highly asymmetric following deflagellation.

*C. reinhardtii* cells also shed their flagella during the cell cycle; however, unlike reflagellating cells, mitotic cells do not regenerate their flagella. In order to determine which changes in nuclear architecture were solely due to flagellar excision, we examined the changes in nuclear architecture during the cell cycle using triple confocal immunofluorescence microscopy. The size of the interphase nucleus varied through the cell cycle, steadily increasing until almost doubling its volume prior to mitotic entry (Figure 5A). The NPCs in mitotic cells were more prevalent in the posterior nuclear hemisphere, as observed in interphase nuclei. At the beginning of mitosis, during the preprophase stage, the cells lost their flagella (data not shown). Flagellar excision was accompanied by a contraction in the centrin fibers and a dramatic change in nuclear shape and position within the cell (Salisbury et al., 1988; Figure 5B). The nucleus moved to the anterior end of the cell and its shape changed from oval to pyriform. These changes were similar to those observed during flagellar excision due to pH shock (Salisbury et al., 1987, 1988; Figure 2). The nucleus remained in a pyriform shape until later mitotic stages, when it adopted a rhomboid shape followed by nuclear fission along the anterior-posterior axis (Figure 5D). Although the shape and volume of the nucleus and nucleolus changed during mitosis, the distribution of the NPCs did not vary during the cell cycle, suggesting that NPC hyperpolarization was specific to flagellar regeneration.

### Upregulated β2-Tubulin Transcripts Accumulate in the Polysome-Rich Cytoplasm Adjacent to the Posterior Nuclear Hemisphere

Our observations of increased surface area of the nucleus at the posterior hemisphere, hyperpolarization of the NPC to the posterior side, and polarization of heterochromatin to the anterior side of the nucleus suggested that nuclear architecture dramatically changed during flagellar biosynthesis. These observations led us to hypothesize that changes in nuclear architecture could affect the cytoplasmic fate of mRNAs. In order to test this idea, we adapted the FISH methods of Femino et al. and Long et al. to *C. reinhardtii* (Femino et al., 1998; Long et al., 1995). We designed and labeled five 50-nucleotide probes against *C. reinhardtii* β2-tubulin mRNA, which is highly upregulated during flagellar biosynthesis (Bernstein et al., 1994; Keller et al., 1984). Prior to flagellar autotomy, our probes decorated a single bright point of fluorescence that was frequently observed in the posterior half of the nucleus (Figure 6A; Figure 6B, panel i). This FISH signal corresponds to a single gene locus for β2-tubulin in this haploid organism (Femino et al., 1998). We also observed very low cytoplasmic β2-tubulin RNA signal in these untreated cells (Figure 6A; Figure 6B, panel i). The transcription site and cytoplasmic signal were not observed when FISH was done on cells using a cocktail of probes against the lacZ gene (Figure 6B, panels ii and iv), in cells that were treated with RNase A (data not shown), or in cells that were hybridized with a cocktail mix that included a 1000-fold excess of unlabeled β2-tubulin probe (data not shown). Deflagellated cells that were allowed to regenerate flagella for 20 and 40 min showed a single nuclear transcription site and a high level of β2-tubulin transcripts in the cytoplasm (Figure 6B, panels iii and v–viii). This observation is consistent with previous reports of increased β2-tubulin mRNA transcription and stability during flagellar biosynthesis (Baker et al., 1984). It was very clear that the cytoplasmic β2-tubulin transcripts localized in clusters adjacent to the posterior end of the nucleus. Interestingly, and concordant with a prior report

(Triemer and Brown, 1974), we observed that ribosome-like structures are very abundant in the cytoplasmic area adjacent to the posterior side of the nucleus (Figure 6C). Thus, the newly synthesized β2-tubulin RNAs localized in the polysome-rich cytoplasm adjacent to where NPCs accumulated. Although we have not proven a causal relationship for these observations, we interpret them in terms of a careful choreographing of nuclear architecture and cytoplasmic function.

## Discussion

The data presented here reveal extensive organization in the nucleus of *C. reinhardtii* and dramatic alteration in its organization during flagellar regeneration. The nuclear architecture of *Chlamydomonas* is organized as a series of concentric spheroids, the innermost being the nucleolus. Surrounding the nucleolus is a spherical compartment that presumably contains the sites of synthesis and processing of pre-messenger RNAs, as evidenced by anti-snRNP staining. This partition is circumscribed by an area devoid of staining, which we presume is the laminar periphery, itself surrounded by the outermost cortex—the nuclear envelope with punctate NPC staining. Heterochromatin is homogeneously distributed as a narrow rim close to the nuclear periphery, adjacent to the nuclear envelope. It is in this outermost cortex where we noted evidence for a unique architecture: NPCs were not distributed evenly, but were more prevalent in the posterior hemisphere of the *C. reinhardtii* nucleus, suggesting nuclear polarity.

The uneven arrangement of NPCs was dramatically augmented during reflagellation, a period of robust transcription necessary for the de novo synthesis of flagellar components (Schloss et al., 1984). Interestingly, NPCs were not the only nuclear components that were dramatically reorganized during reflagellation. Whereas the NPC became preferentially distributed toward the posterior side of the nucleus, the narrow rim of heterochromatin near the nuclear periphery redistributed to the anterior side of the nucleus. These observations suggested to us that nuclear polarity was dynamic and regulated in response to physiological stimuli.

The observed redistribution of heterochromatin represents a dramatic reorganization of the underlying chromatin architecture. Chromosomes occupy distinct regions within the nucleus, and this organization affects the synthesis and processing of transcripts (Marshall et al., 1996). Chromosomal domains are organized into distinct euchromatic and heterochromatic regions, and the positioning of genes in these regions is a tightly regulated process that affects gene expression: active genes preferentially localize to the euchromatic areas and silenced genes to the heterochromatic ones (reviewed by Carmo-Fonseca, 2002; Labrador and Corces, 2002). Our data show that the position of heterochromatin in *Chlamydomonas* is regulated. Given its exclusion from the area of increased NPC and β2-tubulin mRNA concentration, it is possible that its regulated relocalization allows active genes in the euchromatic regions access to the NPC at the posterior side of the nucleus.

Whereas it is clear that nuclear architecture increases the efficiency of nuclear processes (Goldstrohm et al., 2001; Maniatis and Reed, 2002), it is not clear whether there is coordination between nuclear architecture and cytoplasmic processes. A structural relationship cannot be easily discerned unless the cell cytoplasm is polarized and thus provides a spatial frame of reference for the nuclear architecture. Prior to our findings, there were suggestions that nuclei of blastoderm embryos of *Drosophila melanogaster* were polar, with the nucleolus and the chromocenters consistently located apically (Foe and Alberts, 1985; Hiraoka et al., 1989), and it was hypothesized that the correct cytoplasmic location could be determined by nuclear targeting (Davis et al., 1993). However, the initial work that suggested that nuclear polarity might play a role in asymmetric paired rule transcript exit has not been supported by recent data (Bullock and Ish-Horowicz, 2001). The posterior concentration of NPCs in the *C. reinhardtii* nucleus directly suggests a way in which nuclear architecture could affect transcript targeting. Our data imply that the increased density of NPCs in the posterior nuclear hemisphere following flagellar autotomy leads to the observed accumulation of β2-tubulin transcripts in the adjacent cytoplasmic region where polysomes reside. The lack of hyperpolarization during mitosis suggests that hyperpolarization of NPCs is most likely a response to reflagellation, a process that involves massive upregulation and mobilization of gene products involved in flagellar biogenesis (Lefebvre et al., 1978; Remillard and Witman, 1982; Weeks and Collis, 1976). We must assume that newly synthesized β2-tubulin protein is transported around the nucleus to the flagella, where they are shunted to the growing flagellar tips (Kozminski et al., 1993).

Although we have not characterized the mechanisms that could lead to a hyperpolarization of the NPC during reflagellation, at least four distinct, but not mutually exclusive, mechanisms can be invoked to account for our observations. Novel assembly of NPCs and disassembly followed by reassembly of NPCs are two mechanisms that we consider unlikely given the rapidity of observed accumulation of NPCs in the posterior hemisphere. Reduction of surface area of the posterior hemisphere of the nucleus, perhaps by dynamic interactions between the nuclear envelope and the lamina, could lead to the increased NPC density observed during reflagellation. Given the contraction of the nucleus-basal body connector and changes in overall nuclear morphology observed immediately after deflagellation and during reflagellation, it is conceivable that mechanical forces create local changes at the nuclear envelope that could perhaps be responsible for NPC and heterochromatin redistribution. Finally, NPC movement could account for their uneven distribution in the nuclear envelope; this has been shown to occur in *S. cerevisiae* (Bucci and Wente, 1997). *S. cerevisiae* NPCs are not only capable of moving dynamically within the nuclear envelope, but are also known to distribute nonrandomly in high-density clusters (Bucci and Wente, 1997). Whereas it has been hypothesized that the clusters may arise from high local transport activity between the nucleus and the cytoplasm, this has not been addressed experimentally.

Further studies in *C. reinhardtii* should unravel the mechanistic underpinnings for the hyperpolarization of

NPCs and the redistribution of heterochromatin. It remains to be determined whether the change in chromatin distribution during flagellar biogenesis causes an increase in the transcription of selected genes or conversely, whether the upregulation of transcription causes a change in the heterochromatic distribution. Regardless of the mechanism, our data strongly suggest that the changes in nuclear architecture and the upregulation of transcription are tightly linked in *C. reinhardtii*. The causal relationship between NPC redistribution and the localization of β2-tubulin transcripts also remains to be determined. It is possible that NPCs actively redistribute to the posterior end of the nucleus to drive the localization of β2-tubulin transcripts and other mRNAs to the most propitious site of translation. Conversely, processes that direct transcript localization could lead to NPC polarization. Regardless of the model, we can conclude with certainty that the nucleus and cytoplasmic organization are well coordinated in *Chlamydomonas*.

This study provides several insights into the regulation of nuclear architecture in eukaryotes: to our knowledge, it is the first demonstration that NPC distribution might be directly linked to the site of transcript localization, that NPC and heterochromatin distribution can be rearranged in response to physiological stimuli, and that NPC partitioning can be choreographed with cytoplasmic polarity. The FISH and nuclear confocal immunofluorescence techniques we adapted for *C. reinhardtii* should allow the simultaneous visualization of multiple subnuclear compartments, the nuclear transcription site, and the cytoplasmic transcript localization. These, in combination with genetic analysis, should be very useful in studying the functional consequences of nuclear architecture and polarity.

## Experimental Procedures

### Cell Culture

*Chlamydomonas reinhardtii* wild-type cells (CC-125) used in the immunofluorescence studies were obtained from the *Chlamydomonas* Genetics Center (Duke University). The cells used in the FISH studies were kindly provided to us by Dr. Mitch Bernstein (Albert Einstein College of Medicine). The cells were grown in 100 ml of high-salt (HS) medium (Sueoka, 1960) in 500 ml Erlenmeyer flasks under 14/10 hr light/dark cycle at 24°C, and bubbled with 5% $CO_2$ in air while shaking. Cells were used at a density of 1–4 $\times$ $10^6$ cells/ml during the third hour of the light cycle.

### Electron Microscopy

Cells were fixed according to a modification of McDonald (1984) in 3% glutaraldehyde buffered with 10 mM HEPES (pH 7.2) for 2 hr at 4°C. After a buffer wash (10 mM HEPES [pH 7.2]), samples were fixed in 1% osmium tetroxide and 0.8% $K_3Fe(CN)_6$ in 4 mM phosphate buffer (pH 7.2) for 30 min at 4°C. Samples were washed in deionized water, mordanted with 0.15% aqueous tannic acid for 1 min at room temperature, washed with deionized water, and stained with 2% aqueous uranyl acetate for 2 hr in the dark. After washing with deionized water, the samples were dehydrated through an ethanol series, cleared with propylene oxide, and embedded in Poly/Bed 812. Blocks were polymerized at 60°C for 48 hr. Silver sections were collected on copper grids and poststained with aqueous 2% uranyl acetate for 15 min, followed by Reynold's lead citrate for 15 min. Samples were observed and photographed on a Jeol 1200 EX electron microscope.

### Flagellar Amputation and Regeneration

Deflagellation by pH shock and flagellar regeneration were performed as described by Lefebvre (1995). The pH of the HS medium was lowered to 4.5 by adding 0.5 N acetic acid. After less than a minute, the pH was raised to 7.0 by the dropwise addition of 0.5 N KOH, and the cells were harvested in a clinical centrifuge and resuspended in fresh medium to allow flagellar regeneration. During the process of flagellar regeneration, aliquots were removed and fixed at the specified time points.

### Immunofluorescence Microscopy

*Chlamydomonas* cells were prepared for immunofluorescence by modifying the protocol described by Sanders and Salisbury (1995). Briefly, cells were allowed to adhere to poly-L-lysine- (Sigma) or polyethylenimine- (Sigma) coated coverslips, and were then simultaneously fixed and permeabilized by submerging the coverslips in −20°C methanol for 10 min. The samples were rehydrated with three changes of phosphate-buffered saline (PBS), and blocked in normal donkey serum (Jackson ImmunoResearch Laboratories) for 30 min. The blocking buffer was then substituted by the primary antibody. The mAb 414 antibody (BabCO), a monoclonal antibody against an NPC protein, was used at a dilution of 1:400 in normal donkey serum at room temperature. The human antiserum (AW; Dr. J. Keene, Duke University), with specificity against core Sm proteins of snRNPs, was used at a dilution of 1:1000 in normal donkey serum (Lerner et al., 1981). The human antiserum, (Serum 1875hv; Dr. J. Craft, Yale University), with specificity against fibrillarin, was used at a dilution of 1:1000 in normal donkey serum (described in Ochs et al., 1985). The rabbit polyclonal anti-centrin antibody (MC1) was used at a dilution of 1:750 in normal donkey serum. For triple immunofluorescence, a cocktail of the three primary antibodies was prepared according to the dilutions mentioned above, and the samples were left incubating for 1 hr at room temperature. Incubation was followed by three washes of PBS and incubation in the secondary antibody. Cy2-conjugated AffiniPure donkey anti-mouse IgG (Jackson ImmunoResearch Laboratories) was used at a dilution of 1:50 in normal donkey serum. Cy5-conjugated AffiniPure donkey anti-rabbit IgG (Jackson ImmunoResearch Laboratories) was used at a dilution of 1:50 in normal donkey serum. Rhodamine red-X-conjugated AffiniPure donkey anti-human IgG (Jackson ImmunoResearch Laboratories) was used at a dilution of 1:100 in normal donkey serum. For triple immunofluorescence, a cocktail of the three secondary antibodies was prepared according to the dilutions mentioned above, and the samples were left incubating for 45 min at room temperature. Samples were then stained with 4′,6-diamidino-2-phenylindole hydrochloride (DAPI) nucleic acid stain (Molecular Probes), followed by washes in PBS and water. After washing, slides were mounted using the ProLong Antifade kit (Molecular Probes) and observed in a Zeiss LSM-410 confocal microscope. Image analysis on nuclear pore concentration was performed on confocal sections of 29 unmanipulated cells and 34 reflagellating cells by quantifying the concentration of fluorescence produced by Nup 414 staining at the anterior versus the posterior side of the nucleus. The concentration of fluorescence was quantified using Carl Zeiss LSM Firmware and Adobe Photoshop by calculating the average pixel value in random samples of equivalent surface area at the posterior and anterior end of the nuclear envelope.

### Fluorescent In Situ Hybridization

The fluorescent in situ hybridization protocol optimized by the Singer lab for mammalian and yeast cells (Femino et al., 1998; Long et al., 1995) was adapted to *Chlamydomonas reinhardtii*. Five 50-nucleotide probes were designed against *C. reinhardtii* β2-tubulin transcripts:

(1) 5′-CGA TCA CAA GCT CGA GTG GCC TGT GTA GAA GTG GTA GTG ATC TAG GTG TT-3′
(2) 5′-AAA CCA TGA CGG CAA AAA CAT TAT CAA GCA TTG GCT GGG AAC GGC GGT GC-3′
(3) 5′-TAC GAA GAG TTC TTG TTC TGC ACG TTC AGC ATC TGC TCG TCC ACC TCC TT-3′
(4) 5′-GCC TCC ACA CCA AAG CGT CAA ATG GCA ATC ACA TGT CAA GTT GTC TTC AG-3′
(5) 5′-CAG CTG CTA TGG CCT ATC ACA CAA GAG CTA ATC CGA CGA GAT GAA TGT CC-3′

The criteria for probe design were a 50% GC content and minimal

crossreactivity. Probes were synthesized with five modified thymines (amino-modified C6-dT from Glen Research; shown in the sequences in bold) spaced six to ten base pairs from each other. Up to 20 μg of the five-probe cocktail were labeled with a monofunctional reactive Cy3 dye (Amersham Pharmacia Biotech). The labeling reaction was allowed to proceed overnight at room temperature, and the probes were then purified by gel filtration on a G50 column, at all times using RNase-free reagents. Twenty nanograms of probe cocktail was used per hybridization reaction. One hundred-fold of competitor (4 mg/ml of a cocktail of salmon sperm DNA and *E. coli* tRNA) was added to the probe preparation, and the cocktail was then dried in a speed vacuum machine. The dried probe cocktail was resuspended in 10 μl of formamide, and heated for 10 min at 85°C prior to hybridization. *Chlamydomonas* cells were prepared by allowing them to attach to poly-L-lysine-coated coverslips and fixing them in 4% formaldehyde (from 8% stock solution, EM grade, Electron Microscopy Science) to preserve nuclear structure. Fixed cells were subsequently permeabilized by immersion in −20°C methanol for 10 min. This step was repeated with fresh methanol to quench all remaining autofluorescence. Samples were then rehydrated and washed twice in PBS with 5 mM $MgCl_2$. The samples were then washed with 0.5% Triton PBS with 5 mM $MgCl_2$, followed by two more washes in PBS and 5 mM $MgCl_2$. Cells were then equilibrated in 2× SSC with 50% formamide solution and allowed to hybridize overnight at 37°C with the hybridization cocktail (labeled probe with hybridization buffer, consisting of 40 μl of DEPC water, 20 μl of BSA [20 mg/ml], 20 μl of 20× SSC, and 20 μl of vanadyl/ribonucleoside complex). Following hybridization, samples were washed twice in prewarmed (37°C) 1× SSC with 50% formamide solution. This was followed by a series of washes of 1× SSC, 0.5× SSC, and PBS with 5 mM $MgCl_2$. The cells were then stained with DAPI nucleic acid stain (Molecular Probes), followed by a wash in PBS and 5 mM $MgCl_2$. Coverslips were mounted in 90% glycerol, PBS, 1 mg/ml p-phenylenediamine, and the slides were stored at −20°C until imaging. Cell imaging and analysis for FISH was done as described previously (Femino et al., 1998; Matthiesen et al., 2001).

## Acknowledgments

This work was supported by grant AI40875 to M.A.G.-B. (supplement for training of D.A.C.-R.); grant GM54887 to R.H.S.; grant CA72836 to J.L.S.; a Josiah Macy Foundation fellowship of the Marine Biological Laboratory to M.A.G.-B.; and an Anita Zorzoli, Ph.D. Memorial Fund research award of the Marine Biological Laboratory to D.A.C.-R. M.A.G.-B. also thanks Mr. and Mrs. Arthur D. Lionberger for support. We thank Steve Braut and Jeff Levsky for help with FISH and imaging. We thank Rick Fehon, Elizabeth Harris, Charles Hauser, Mitch Bernstein, Eric Wagner, Bryan Cullen, and Javier Irazoqui for stimulating discussions and reagents. We also thank Wallace Marshall and Joel Rosenbaum for enlightening discussions.

Received: August 6, 2002
Revised: March 5, 2003
Accepted: April 16, 2003
Published: June 2, 2003

## References

Baker, E.J., Schloss, J.A., and Rosenbaum, J.L. (1984). Rapid changes in tubulin RNA synthesis and stability induced by deflagellation in *Chlamydomonas*. J. Cell Biol. *99*, 2074–2081.

Baker, E.J., Keller, L.R., Schloss, J.A., and Rosenbaum, J.L. (1986). Protein synthesis is required for rapid degradation of tubulin mRNA and other deflagellation-induced RNAs in *Chlamydomonas reinhardi*. Mol. Cell. Biol. *6*, 54–61.

Bernstein, M., Beech, P.L., Katz, S.G., and Rosenbaum, J.L. (1994). A new kinesin-like protein (Klp1) localized to a single microtubule of the *Chlamydomonas* flagellum. J. Cell Biol. *125*, 1313–1326.

Blobel, G. (1985). Gene gating: a hypothesis. Proc. Natl. Acad. Sci. USA *82*, 8527–8529.

Brennan, C.M., and Steitz, J.A. (2001). HuR and mRNA stability. Cell. Mol. Life Sci. *58*, 266–277.

Bucci, M., and Wente, S.R. (1997). In vivo dynamics of nuclear pore complexes in yeast. J. Cell Biol. *136*, 1185–1199.

Bullock, S.L., and Ish-Horowicz, D. (2001). Conserved signals and machinery for RNA transport in *Drosophila* oogenesis and embryogenesis. Nature *414*, 611–616.

Carmo-Fonseca, M. (2002). The contribution of nuclear compartmentalization to gene regulation. Cell *108*, 513–521.

Davis, I., Francis-Lang, H., and Ish-Horowicz, D. (1993). Mechanisms of intracellular transcript localization and export in early *Drosophila* embryos. Cold Spring Harb. Symp. Quant. Biol. *58*, 793–798.

Dundr, M., and Misteli, T. (2001). Functional architecture in the cell nucleus. Biochem. J. *356*, 297–310.

Femino, A.M., Fay, F.S., Fogarty, K., and Singer, R.H. (1998). Visualization of single RNA transcripts in situ. Science *280*, 585–590.

Foe, V.E., and Alberts, B.M. (1985). Reversible chromosome condensation induced in *Drosophila* embryos by anoxia: visualization of interphase nuclear organization. J. Cell Biol. *100*, 1623–1636.

Gall, J.G. (2001). A role for Cajal bodies in assembly of the nuclear transcription machinery. FEBS Lett. *498*, 164–167.

García-Blanco, M.A., Miller, D.D., and Sheetz, M.P. (1995). Nuclear spreads: I. Visualization of bipartite ribosomal RNA domains. J. Cell Biol. *128*, 15–27.

Goldstrohm, A.C., Greenleaf, A.L., and García-Blanco, M.A. (2001). Co-transcriptional splicing of pre-messenger RNAs: considerations for the mechanism of alternative splicing. Gene *277*, 31–47.

Gu, W., Pan, F., Zhang, H., Bassell, G.J., and Singer, R.H. (2002). A predominantly nuclear protein affecting cytoplasmic localization of β-actin mRNA in fibroblasts and neurons. J. Cell Biol. *156*, 41–51.

Harris, E.H. (1989). The *Chlamydomonas* Sourcebook (San Diego, CA: Academic Press).

Hiraoka, Y., Minden, J.S., Swedlow, J.R., Sedat, J.W., and Agard, D.A. (1989). Focal points for chromosome condensation and decondensation revealed by three-dimensional in vivo time-lapse microscopy. Nature *342*, 293–296.

Holmes, J.A., and Dutcher, S.K. (1989). Cellular asymmetry in *Chlamydomonas reinhardtii*. J. Cell Sci. *94*, 273–285.

Johnson, U.G., and Porter, K.R. (1968). Fine structure of cell division in *Chlamydomonas reinhardtii*. J. Cell Biol. *38*, 403–425.

Keller, L.R., Schloss, J.A., Silflow, C.D., and Rosenbaum, J.L. (1984). Transcription of α- and β-tubulin genes in vitro in isolated *Chlamydomonas reinhardi* nuclei. J. Cell Biol. *98*, 1138–1143.

Kozminski, K.G., Johnson, K.A., Forscher, P., and Rosenbaum, J.L. (1993). A motility in the eukaryotic flagellum unrelated to flagellar beating. Proc. Natl. Acad. Sci. USA *90*, 5519–5523.

Labrador, M., and Corces, V.G. (2002). Setting the boundaries of chromatin domains and nuclear organization. Cell *111*, 151–154.

Lawrence, J.B., Singer, R.H., and Marselle, L.M. (1989). Highly localized tracks of specific transcripts within interphase nuclei visualized by in situ hybridization. Cell *57*, 493–502.

Lefebvre, P.A. (1995). Flagellar amputation and regeneration in *Chlamydomonas*. Methods Cell Biol. *47*, 3–7.

Lefebvre, P.A., Nordstrom, S.A., Moulder, J.E., and Rosenbaum, J.L. (1978). Flagellar elongation and shortening in *Chlamydomonas*. IV. Effects of flagellar detachment, regeneration, and resorption on the induction of flagellar protein synthesis. J. Cell Biol. *78*, 8–27.

Leger-Silvestre, I., Trumtel, S., Noaillac-Depeyre, J., and Gas, N. (1999). Functional compartmentalization of the nucleus in the budding yeast *Saccharomyces cerevisiae*. Chromosoma *108*, 103–113.

Lerner, M.R., Boyle, J.A., Hardin, J.A., and Steitz, J.A. (1981). Two novel classes of small ribonucleoproteins detected by antibodies associated with lupus erythematosus. Science *211*, 400–402.

Long, R.M., Elliott, D.J., Stutz, F., Rosbash, M., and Singer, R.H. (1995). Spatial consequences of defective processing of specific yeast mRNAs revealed by fluorescent in situ hybridization. RNA *1*, 1071–1078.

Long, R.M., Gu, W., Meng, X., Gonsalvez, G., Singer, R.H., and Chartrand, P. (2001). An exclusively nuclear RNA-binding protein

affects asymmetric localization of ASH1 mRNA and Ash1p in yeast. J. Cell Biol. *153*, 307–318.

Mahy, N.L., Perry, P.E., Gilchrist, S., Baldock, R.A., and Bickmore, W.A. (2002). Spatial organization of active and inactive genes and noncoding DNA within chromosome territories. J. Cell Biol. *157*, 579–589.

Maniatis, T., and Reed, R. (2002). An extensive network of coupling among gene expression machines. Nature *416*, 499–506.

Marshall, W.F., Dernburg, A.F., Harmon, B., Agard, D.A., and Sedat, J.W. (1996). Specific interactions of chromatin with the nuclear envelope: positional determination within the nucleus in *Drosophila melanogaster*. Mol. Biol. Cell *7*, 825–842.

Matthiesen, S.H., Shenoy, S.M., Kim, K., Singer, R.H., and Satir, B.H. (2001). A parafusin-related *Toxoplasma* protein in $Ca^{2+}$-regulated secretory organelles. Eur. J. Cell Biol. *80*, 775–783.

McDonald, K. (1984). Osmium ferricyanide fixation improves microfilament preservation and membrane visualization in a variety of animal cell types. J. Ultrastruct. Res. *86*, 107–118.

Ochs, R.L., Lischwe, M.A., Spohn, W.H., and Busch, H. (1985). Fibrillarin: a new protein of the nucleolus identified by autoimmune sera. Biol. Cell *54*, 123–133.

Remillard, S.P., and Witman, G.B. (1982). Synthesis, transport, and utilization of specific flagellar proteins during flagellar regeneration in *Chlamydomonas*. J. Cell Biol. *93*, 615–631.

Rosenbaum, J.L., Moulder, J.E., and Ringo, D.L. (1969). Flagellar elongation and shortening in *Chlamydomonas reinhardtii*. J. Cell Biol. *41*, 600–619.

Ryan, K.J., and Wente, S.R. (2000). The nuclear pore complex: a protein machine bridging the nucleus and cytoplasm. Curr. Opin. Cell Biol. *12*, 361–371.

Sager, R., and Palade, G.E. (1957). Structure and development of the chloroplast in *Chlamydomonas*. I. The normal green cell. J. Biophys. Biochem. Cytol. *3*, 463–487.

Salisbury, J.L., Baron, A., Surek, B., and Melkonian, M. (1984). Striated flagellar roots: isolation and partial characterization of a calcium-modulated contractile organelle. J. Cell Biol. *99*, 962–970.

Salisbury, J.L., Sanders, M.A., and Harpst, L. (1987). Flagellar root contraction and nuclear movement during flagellar regeneration in *Chlamydomonas reinhardtii*. J. Cell Biol. *105*, 1799–1805.

Salisbury, J.L., Baron, A.T., and Sanders, M.A. (1988). The centrin-based cytoskeleton of *Chlamydomonas reinhardtii*: distribution in interphase and mitotic cells. J. Cell Biol. *107*, 635–641.

Sanders, M.A., and Salisbury, J.L. (1995). Immunofluorescence microscopy of cilia and flagella. Methods Cell Biol. *47*, 163–169.

Schloss, J.A., Silflow, C.D., and Rosenbaum, J.L. (1984). mRNA abundance changes during flagellar regeneration in *Chlamydomonas reinhardtii*. Mol. Cell. Biol. *4*, 424–434.

Schotz, F., Bathelt, H., Arnold, C.G., and Schimmer, O. (1972). Protoplasma *75*, 229–254.

Sueoka, N. (1960). Mitotic replication of deoxyribonucleic acid in *Chlamydomonas reinhardtii*. Proc. Natl. Acad. Sci. USA *46*, 83–91.

Triemer, R.E., and Brown, R.M.J. (1974). Cell division in *Chlamydomonas moewusii*. J. Phycol. *10*, 419–433.

Weeks, D.P., and Collis, P.S. (1976). Induction of microtubule protein synthesis in *Chlamydomonas reinhardi* during flagellar regeneration. Cell *9*, 15–27.

Weiss, D., Schneider, G., Niemann, B., Guttmann, P., Rudolph, D., and Schmahl, G. (2000). Computed tomography of cryogenic biological specimens based on X-ray microscopic images. Ultramicroscopy *84*, 185–197.

Wilkie, G.S., Shermoen, A.W., O'Farrell, P.H., and Davis, I. (1999). Transcribed genes are localized according to chromosomal position within polarized *Drosophila* embryonic nuclei. Curr. Biol. *9*, 1263–1266.

Wright, R.L., Salisbury, J., and Jarvik, J.W. (1985). A nucleus-basal body connector in *Chlamydomonas reinhardtii* that may function in basal body localization or segregation. J. Cell Biol. *101*, 1903–1912.

Zhang, G., Taneja, K.L., Singer, R.H., and Green, M.R. (1994). Localization of pre-mRNA splicing in mammalian nuclei. Nature *372*, 809–812.